Original Article

Reversal of heavy arterial calcification in a rat model of chronic kidney disease using targeted ethylene diamine tetraacetic acid-loaded albumin nanoparticles

Fatema Tuj Zohora[1], Shivani Arora[1], Alyssa Swiss[2], Naren Vyavahare[1]

[1]Department of Bioengineering, Clemson University, Clemson, SC, USA; [2]Elastrin Therapeutics Inc., Greenville, SC, USA

Contributions: (I) Conception and design: N Vyavahare, FT Zohora, S Arora; (II) Administrative support: N Vyavahare; (III) Provision of study materials or patients: N Vyavahare; (IV) Collection and assembly of data: FT Zohora, S Arora; (V) Data analysis and interpretation: FT Zohora, S Arora; (VI) Manuscript writing: All authors; (VII) Final approval of manuscript: All authors.

Correspondence to: Naren Vyavahare, PhD. Hunter Endowed Chair and Professor, Department of Bioengineering, Clemson University, 501 Rhodes Hall, Clemson, SC 29634, USA. Email: narenv@clemson.edu.

Background: Elastin degradation and severe calcification in the medial layer of the vessel wall, known as medial arterial calcification (MAC), is typical in the aging population and patients with metabolic disorders, such as diabetes and chronic kidney disease (CKD). We have previously reported that ethylene diamine tetraacetic acid (EDTA) delivery to the site of calcification can be achieved by tagging nanoparticles with an elastin antibody that recognizes explicitly damaged elastin, and such systemic therapy can remove focal calcium deposits from the calcified arteries in CKD rodent model. The current study aims to test whether heavy calcification seen throughout arterial tree and kidneys in CKD can be reversed with nanoparticle therapy.

Methods: Thirty healthy male Sprague-Dawley rats weighing approximately 300 g, were placed on an adenine diet for 21 non-consecutive days to induce kidney failure, followed by daily vitamin D3 (VitD3) injections for 4 sequential days to cause severe calcification throughout the cardiovascular system and kidneys. DiR-dye loaded and elastin antibody conjugated albumin nanoparticles were used to confirm the targeting of nanoparticles to the calcification area. The rats were divided into two groups for targeted removal of calcification starting at day 7 of the last doses of VitD3. The experimental group received biweekly IV injections of anti-elastin antibody conjugated EDTA loaded human serum albumin nanoparticles (EDTA-HSA-El-Ab NPs), while the sham controls received blank nanoparticles (Blank-HSA-El-Ab NPs) (5 injections in total). Micro-computed tomography (microCT) was used to analyze the extent of calcification. Reverse transcription polymerase chain reaction (RT-PCR) and immunohistochemistry studies were performed for osteogenic markers, including bone morphogenic protein 2 (BMP2), runt-related transcription factor 2 (RUNX2), and tissue non-specific alkaline phosphatase (TNAP). For comparison, aortic ring organ cultures from healthy rats were treated with high phosphate to induce calcification *in vitro*, and then they were treated with EDTA. Human calcified femoral arteries were also treated *ex vivo* with EDTA-HSA-EL-Ab NPs to test if nanoparticles remove heavy calcification.

Results: EDTA-loaded nanoparticles that specifically target degraded elastin reversed existing heavy mineral deposits in arteries, as per elemental calcium analysis (124.161±34.410 µg Ca per mg of the dry aorta in Blank-HSA-El-Ab NPs *vs.* 100.520±19.131 µg in EDTA-HSA-El-Ab NPs group, P=0.04) and microCT (object volume, 129.001±37.785 *vs.* 29.815±24.169 mm^3, P=0.0005). The reversal of aortic calcification was accompanied by a significant reduction of bone-associated mRNA expression of *BMP2* and *RUNX2* (P=0.01). Immunohistochemistry studies corroborated RT-PCR results, showing a reduction of BMP2 and RUNX2 stains in the vessel wall. The rat aortic ring culture study also showed similar results, where osteogenic genes (*BMP2*, *RUNX2*) and proteins (BMP2, RUNX2, TNAP) were suppressed upon reversal of calcification with EDTA (P=0.001). We also show *ex vivo* reversal of human femoral artery calcification by microCT (calcium intensity: untreated, 57.721±28.551 *vs.* day 6 of treatment, 5.441±3.615, P=0.01) by EDTA nanoparticle therapy.

Conclusions: This is the first study showing the removal of calcium from heavily calcified arteries by using intravenous targeted EDTA therapy. Such therapy also reversed vascular smooth muscle cell osteoblastic transition and apoptosis in the arterial tissue, thereby potentially creating an environment for suitable tissue repair.

Keywords: Vascular calcification; chronic kidney disease (CKD); ethylene diamine tetraacetic acid targeted delivery (EDTA targeted delivery); elastin damage; antibody targeting

Submitted Jan 07, 2024. Accepted for publication Jul 03, 2024. Published online Aug 23, 2024.
doi: 10.21037/cdt-24-17
View this article at: https://dx.doi.org/10.21037/cdt-24-17

Introduction

Elastin-associated medial arterial calcification (MAC), characterized by ectopic calcium deposition in arteries, is a significant risk factor for cardiovascular morbidity and mortality (1). Calcification causes hardening of arteries as well as aortic valves, leading to stiffening and resistance to blood flow that increases cardiac work and, ultimately, heart failure (2). Diverse etiologies involving mineral imbalances, uremic toxins, and pathologic deficiencies or genetic mutations in calcification inhibitors lead to either initiation or growth of hydroxyapatite mineral formation on damaged elastic fibers in the medial layer of the vessel wall (2,3). A genetic condition known as generalized arterial calcification in infancy (GACI) that occurs due to mutations in eNPP1 and ABCC6 also causes severe calcification in large and medium-sized elastic arteries (4,5).

Tissue-specific microenvironmental factors and signaling pathways like oxidative stress, hyperglycemia, and dysregulated calcium and phosphate (Pi) balance govern the mineralization process in arteries during aging, atherosclerosis, and chronic kidney disease (CKD). Medial arterial calcification is the most common form of vascular mineralization observed in the aging population and patients with metabolic diseases like diabetes and CKDs. Reports from many researchers, including us, have evidenced the role of dysregulated calcium and Pi balance in precipitating osteogenic differentiation of vascular smooth muscle cells (VSMCs) (6,7). We have previously shown that rat smooth muscle cells (SMCs) when cultured on calcified elastin and hydroxyapatite matrix, undergo osteoblastic transition via BMP-2/SMAD-5 signaling pathway with a simultaneous increase in Ca sensing receptor (CaSR) density on VSMCs (8). We have also shown that ethylene diamine tetraacetic acid (EDTA)-loaded albumin nanoparticles, tagged with an anti-elastin antibody that recognizes explicitly damaged elastin, can deliver EDTA to calcification sites close to elastin degradation and remove focal calcium deposits from the calcified arteries in the adenine diet-induced rat CKD model of MAC (9). In that study, a few spots of calcifications were regressed with our therapy. In CKD patients, the whole arterial tree gets heavily calcified, and patient mortality is caused by vascular failure rather

Highlight box

Key findings

- This study shows that systemic chelation therapy with targeted ethylenediamine tetra acetic acid loaded albumin nanoparticles (EDTA-HSA-El-Ab NPs) can potentially regress heavy arterial calcification with the suppression of osteogenic phenotypes in vascular cells.

What is known, and what is new?

- Damaged elastin targeted EDTA-loaded albumin nanoparticles have been demonstrated in previous studies to successfully reverse locally induced arterial calcification or systemic mild calcification without inducing side effects on bones or kidneys observed with systemic chelation therapy.
- Here, we report the same nanoparticle formulation to reverse systemically induced heavy arterial calcification in an animal model resembling calcification status in patients with advanced stage chronic kidney disease (CKD).

What is the implication, and what should change now?

- Targeted EDTA therapy can reverse not only heavy arterial calcification but also reverse osteoblastic transition and apoptosis in the arterial cells, thereby potentially creating an environment for suitable tissue repair.
- Such intravenous therapy can help to reduce cardiovascular events in CKD patients. Further studies will determine the dosage required for nearly complete calcification removal and to what degree of reversal is necessary to prevent cardiovascular disease progression.

than kidney failure. The Adenine rat model is established to cause focal arterial calcification by depositing adenine metabolite crystals in kidney tubules and resulting renal function impairment that takes long period to develop. To accelerate the calcification process and to mimic heavy calcification throughout arterial tree as observed in CKD patients, we combined the adenine diet and vitamin D3 (VitD3) administration. High doses of VitD3 causes vascular calcification via disrupting endogenous calcification regulating systems, including parathyroid hormone-related peptide, and by accelerating intestinal absorption of calcium and phosphorous that leads to hypercalcemia and hyperphosphatemia (10,11). This model eliminates the complexity of traditional 5/6 nephrectomy that requires surgical procedures. In separate experiments, aortic rings from normal rats were cultured under high Pi conditions to induce arterial calcification *in vitro*. We show that targeted EDTA nanoparticle therapy not only removes calcific deposits but also reverses the process of osteogenic differentiation, as is evident by decreased expression of bone markers, such as bone morphogenic protein 2 (BMP2), runt-related transcription factor 2 (RUNX2), and tissue non-specific alkaline phosphatases (TNAP) at both transcriptional and translational level. Further, it decreased the expression of caspase-3, an apoptotic marker, in the aorta. We present this article in accordance with ARRIVE reporting checklist (available at https://cdt.amegroups.com/article/view/10.21037/cdt-24-17/rc).

Methods

Preparation of anti-elastin antibody conjugated EDTA-loaded human serum albumin nanoparticles (EDTA-HSA-El-Ab NPs) for targeted delivery

EDTA-HSA-El-Ab NPs were fabricated by the ethanol desolvation method, as described in earlier studies with a slight modification (9). Briefly, 200 mg of human serum albumin (HSA) (SeraCare, Milford, MA, USA) was dissolved in 4 mL of deionized water, and 50 mg of disodium EDTA (Fisher Scientific, NJ, USA) was then dissolved in HSA solution. The pH of the mixture was adjusted to approximately 8.5 with 6N NaOH. The solution was then added dropwise to the absolute ethanol (Sigma, St. Louis, MO, USA) (1 mL/min) under constant stirring, followed by the addition of 25 µL of 8% glutaraldehyde as a crosslinker. Crosslinking of nanoparticles was continued for 2 hours at room temperature under constant stirring at 800 rpm. Formulated nanoparticles were then separated by centrifugation at 6,000 rpm for 10 minutes, rinsed in deionized water (saturated with EDTA), and resuspended in Pi-buffered saline to proceed to anti-elastin antibody conjugation as detailed previously (9,12). Briefly, 10 mg of formulated nanoparticles were PEGylated with 2.5 mg of α-maleimide-ω-N-hydroxysuccinimide ester poly (ethylene glycol) (mPEGNHS, MW 2000, Nanocs, NY, USA) for an hour at room temperature under gentle agitation. Meanwhile, 20 µg of custom-made humanized anti-elastin antibody called 'Flexibzumab' was added to 68 µg of Traut's reagent (G-Biosciences, Saint Louis, MO, USA) for antibody thiolation. Subsequently, the mixture was incubated in 4-(2-hydroxyethyl)-1-piperazineethanesulfonic acid (HEPES) buffer (20 mM, pH =8.8) at room temperature for an hour under gentle agitation. Finally, thiolated antibody was added to the PEGylated nanoparticles and incubated overnight (16 hours) at 4 ℃ under gentle rocking for conjugation.

Preparation of anti-elastin antibody conjugated DiR-dye loaded human serum albumin nanoparticles (DiR-HSA-El-Ab NPs) for targeting studies

DiR (1,1-dioctadecyl-3,3,3,3-tetramethylindotricarbocyanineiodide) (PromoCell GmbH, Heidelberg, Germany) dye-loaded HSA nanoparticles were prepared by using ethanol desolvation method and conjugated with humanized ani-elastin antibody for targeting studies as described earlier (13). In short, 250 mg of HSA was dissolved in 4 mL of deionized water, and 2.5 mg of DiR-dye was dissolved in acetone. DiR-dye was then added to the HSA solution dropwise and stirred at room temperature for about an hour, following which glutaraldehyde (EM grade 70%, EMS, PA, USA) was added to the mixture at a concentration of 42 µg/mg of HSA for crosslinking. The mixture was then added dropwise to 24 mL of ethanol under continuous sonication on ice and kept for 30 minutes for nanoparticle formation. DiR-loaded HSA nanoparticles were then isolated by centrifugation at 4,000 rpm for 10 minutes, washed with water, and resuspended in Pi-buffered saline for anti-elastin antibody conjugation.

Experimental rodent model of CKD with severe arterial calcification

Animal experiments were approved by the Institutional Animal Care and Use Committee (IACUC) at Clemson

University (animal use protocol number 2021-006), in compliance with institutional guidelines for the care and use of animals. A protocol has been prepared before the study without registration. Male Sprague-Dawley rats (weighing approx. 250 g, and age 11–12 weeks) obtained from Charles River Laboratories were acclimatized for 2 weeks before starting the study and were maintained on a standard rodent diet (Teklad Global 18% Protein Rodent Diet; Inotiv, Madison, WI, USA). The animals were randomly divided into treatment groups and control groups (n=34 in total). Control group animals (n=4) were maintained on a standard chow diet till the completion of the study, and the animals in the treatment groups (n=30) were maintained on 0.75% adenine diet containing 2.5% protein (TD. 130127; Inotiv) with a modified schedule for 21 days as described previously (9). Seven days after completion of the adenine diet, the animals in the treatment groups were either injected intraperitoneally with VitD3 (8.75 mg/kg/day formulated in olive oil) or equivalent olive oil as a vehicle for 4 consecutive days. The animals that received olive oil following 21 days of the adenine diet formed the Adenine diet-only group (n=4). Two rats from adenine and VitD3 group were used to study targeting of damaged aortic elastin and calcification progression by targeted DiR-HSA-El-Ab NPs and micro-computed tomography (microCT) upon sacrifice. Two animals died at the beginning of therapeutic study and were withdrawal from the study. The rest of the animals (n=22) in the treatment group that received VitD3 injections were further randomly subdivided into two groups: (I) the EDTA-treated group (named EDTA-HSA-El-Ab NPs, n=11)—in which the animals received 2 weekly injections (a total of 5 injections) of EDTA-HSA-El-Ab NPs (10 mg/kg IV), and (II) the blank NP group (named Blank-HSA-El-Ab NPs, n=11)—in which the animals received Blank-HSA-El-Ab NPs with same dosage as EDTA nanoparticles. Following confirmation of targeting and aortic calcification with DiR-HSA-El-Ab NPs, the nanoparticle therapy with Blank/EDTA started at day 7 of the last doses of VitD3. After 3 weeks of Blank/EDTA nanoparticle therapy, the aortas (from the heart to the iliac bifurcation) and other organs, including lungs, liver, kidneys, and spleen, were harvested and preserved accordingly for further analysis. Blood was also collected for serum isolation and biomarker analysis. During the entire study, the animals were monitored for body weight, temperature, and regular activities by an experienced veterinarian and were euthanized by saline perfusion under isoflurane anesthesia when they reached a humane endpoint of >25% weight loss and clinical signs of suffering (according to IACUC guidelines on humane endpoints), that includes very little food/water intake, no grooming, less movement/gating, becoming scruffy, shaky, back arching, cold body temperature, and porphyrin secretion. The animals were housed with a periodic 12 hours of dark and light cycle, with room temperature and humidity of 68–70 °F and 35–45%, respectively. However, a heating pad (37 °C) was provided underneath, covering half of the cage's bottom when the body temperature fell due to sickness.

Targeting efficacy of anti-elastin antibody conjugated nanoparticles

Two rats from the same cohort mentioned in the previous section that were fed adenine and administered VitD3 were used to analyze *in vivo* targeting. Ten mg/kg of DiR-HSA-El-Ab NPs were administered via the tail vein 5 days after the last dose of VitD3 injections. Following 24 hours of DiR targeting, rats were euthanized by saline perfusion under isoflurane anesthesia, and organs were harvested for fluorescent and microCT imaging in *ex vivo*. The targeting of DiR-HSA-El-Ab NPs was visualized with Caliper IVIS Lumina XR (Hopkinton, MA, USA) with Ex/Em of 745/795 nm. To confirm the coexistence of DiR-HSA-El-Ab signaling with calcification, aortas were imaged for calcification using microCT (Skyscan 1176, Bruker BioSpin, Billerica, MA, USA).

Ex vivo calcification studies with rat aortic rings

In a separate study, a new cohort of healthy male Sprague-Dawley rats (approximately 450 g, n=6) were euthanized by saline perfusion under isoflurane anesthesia for harvesting full-length aortas. Aortas were collected in an aseptic condition in ice-cold Moscona's buffer (8 g NaCl, 0.2 g KCl, 1 g $NaHCO_3$, 1.7 g glucose, 0.005 g NaH_2PO_4 in 1 L DI water; pH 7.2) to carry to the lab. After washing four times with Dulbecco's phosphate buffered saline (PBS), the aortas from ascending to the iliac bifurcation were cut into pieces to obtain 3–4 mm aortic rings. These rings were then cultured in low glucose Dulbecco's modified eagle medium (DMEM) with 1% heat-inactivated fetal bovine serum (FBS) and 1% penicillin-streptomycin in a humidified incubator at 37 °C, under 5% CO_2 for overnight equilibration. Afterward, the aortic rings were treated with 0.5 U/mL elastase for 40 minutes at 37 °C

for aortic elastin degradation, which has been found to help in heavy aortic calcification when cultured in a high Pi medium. Subsequently, elastase-treated aortic rings were washed twice with PBS and incubated in high Pi medium in DMEM (final concentration of Pi: 2.9 mM) containing 1% heat-inactivated FBS and 1% penicillin-streptomycin for 10 days onwards. After establishing heavy aortic calcification as observed via microCT scan, the rings were then cultured with 0.5 mg/mL pure Na_2EDTA (this corresponds to the same concentration as delivered *in vivo* with HSA nanoparticles) in the presence of high Pi in DMEM along with 10% FBS for 6 more days till the end of the experiment. The experimental groups (n=3 per group) are: (I) DMEM only (0.9 mM Pi; denoted as a control group); (II) elastase & high Pi treated with no Na_2EDTA (named, Pi group); (III) elastase & high Pi treated followed by Na_2EDTA (Pi + EDTA group). In this study, Pi was provided as $NaH_2PO_4{\cdot}2H_2O$ to obtain a final concentration of 2.9 mM. During incubation, the conditioned medium was replaced every 2 days.

Analysis of blood biochemical parameters

Blood samples were collected via cardiac puncture before saline perfusion. Collected samples were kept at room temperature for approximately 40 minutes to allow clotting. Clotted blood was then centrifuged at 400 g for 20 minutes to separate serum. Isolated serum samples were aliquoted and kept at −80 ℃ before being sent to AnMed Health (Anderson, SC, USA) to analyze serum biomarkers—calcium, phosphorous, creatinine, and alkaline phosphatase (ALP).

MicroCT imaging for calcification

Calcification or mineral deposits in rat aortas and kidneys were scanned using microCT (Bruker Skyscan 1176, Billerica, MA, USA). Immediately after sacrifice, rat aortas were explanted and kept in cold PBS in 50 mL tubes for microCT scanning. Aortic scanning was performed using a 0.5 mm Aluminum filter, at a voltage of 90 kV, and a current of 278 µA, with 45 ms exposure time. Whole kidneys fixed in buffered formalin were scanned using a voltage of 90 kV, a current of 278 µA, with a 0.2 mm Aluminum filter and 55 ms exposure. Both aorta and kidney specimens were scanned using a 360° rotation with a step of 0.7°. The reconstruction of X-ray back-projection images into cross sections was performed using Bruker's NRecon Software, which uses modified Feldkamp's algorithms. The range of attenuation coefficients was same across all aortas or kidneys to acquire a comparable result between Blank-HSA-El-Ab NPs and EDTA-HSA-El-Ab NPs groups. For comparative analysis, Bruker's volume rendering CTVox software was then used to represent reconstructed images as a 3D object, with the same settings over aortas or kidneys. Further, 3D morphometric analysis was conducted with CTAn software from Bruker.

Elemental calcium quantification by ICP-MS

To quantify total calcium content in aortic segments from animal study, lyophilized tissues were digested in 6N HCl for overnight at 95 ℃. Following complete digestion, HCl evaporated under a continuous stream of N_2 gas for approximately 30 minutes. The dried remnants were then reconstituted in 0.01N HCl for analysis with Spectro Acros ICP Spectrometer (SPECTRO Analytical Instruments, Kleve, Germany) at Clemson University Agricultural Service Laboratory. The calcium concentration in tissue extracts from individual aortic segments were normalized to the corresponding lyophilized weights and expressed as microgram calcium per milligram of dry aorta.

Alizarin red staining for aortic calcification

Optimal cutting temperature (OCT) compound-embedded frozen sections (10 µm each) were stained with 2% alizarin red solution (pH 4.1–4.3) for 45 seconds. The stained sections were then washed with two changes of distilled water for 10 minutes each and subsequently dehydrated in graded alcohol and xylene for mounting and bright field imaging with Keyence BZ-810. Semi-quantitative analysis for percentage positive stain was performed with four to six serial sections equally distributed from each abdominal aortic sample.

Kidney histology

Kidneys were fixed in 10% neutral buffered formalin first. A cross-section of formalin-fixed kidneys was embedded in paraffin and cut into 5 µm sections for mounting on glass slides. The slides were then incubated overnight at 56 ℃ for tissue adherence and dehydration. Afterward, the tissue sections on glass slides were deparaffinized and rehydrated using xylene and graded alcohol. The sections were then stained with hematoxylin and eosin for morphological changes in tissue structure. Kidney slides were also stained

with alizarin red and Masson's trichrome to visualize calcium ions and collagen deposition, respectively.

Immunohistochemical (IHC) analysis of the aorta

Abdominal aortas with cryosections of 10 µm thickness were fixed in cold acetone for 10 minutes, followed by rehydration along with decalcification in 0.5% of disodium EDTA in Dulbecco's PBS for 15 minutes at room temperature. The sections were then washed in PBS and subsequently blocked with Background Buster for 30 minutes at room temperature and incubated at 4 ℃ overnight with primary antibodies: Rabbit anti-Rat Caspase-3 (Cell Signaling Technology, Danvers, MA, USA), BMP-2, RUNX2, TNAP, and PiT-1 (Santa Cruz Biotechnology, Dallas, TX, USA). Stained sections were then incubated with appropriate secondary antibodies conjugated with Alexa flour 594 or Cy5 to visualize the target proteins. Finally, the aortic sections were counterstained with DAPI and mounted with an aqueous mounting medium for imaging. Four to six sections of equal spacings were taken from each sample for the semi-quantitative analysis of target proteins.

ALP activity assay

SensoLyte pNPP Alkaline Phosphatase Assay Kit (AnaSpec, Fremont, CA, USA) was used to read absorbance at 405 nm per manufacturer's instructions to detect ALP activity in tissues or conditioned medium. Shortly, 50 µL of tissue-extracted proteins or conditioned medium were mixed with 50 µL of pNPP substrate solution in a 96-well flat bottom plate to detect ALP. The mixture turns yellow following 60 minutes of incubation at room temperature due to the dephosphorylation of pNPP. The absorbance was read at 405 nm, and ALP concentration was quantified through a standard calibration curve. The data were normalized by correcting the total protein content and expressing ALP in nanograms per milligram of total protein.

Reverse transcriptase quantitative polymerase chain reaction (RT-qPCR) for gene expression

The expression of genes of interest was performed in aorta samples. The tissue was stored immediately after retrieval in the Trizol. The tissue was homogenized in Trizol using Powergen 125 (FS-PG125, Fisher Scientific) homogenizer, and RNA was extracted using the phenol-chloroform extraction method. A Nanodrop instrument was used to analyze the extracted RNA through quantitative and qualitative analysis. cDNA synthesis was performed using 200 ng of total RNA with iScript gDNA clear cDNA synthesis Kit (Cat# 1725034, Bio-Rad, Laboratories, Inc., Hercules, CA, USA). The total cDNA obtained was diluted five times before amplification with iTaq-Universal SYBR Green Supermix reagent (Cat# 172512, Bio-Rad) on Bio-Rad quantitative PCR platform (96-well format). Quantification was performed using the delta-delta C_T method, using HPRT1 as a housekeeping gene. A list of Primers used in the study is given in Table S1.

Decalcification of human arteries with EDTA-HSA-El-Ab NPs in ex vivo

EDTA-HSA-El-Ab NPs with 30 mg of particles were resuspended in 2 mL of PBS. For resuspension, the nanoparticles were sonicated briefly, then vortexed, and then sonicated again. Heavily calcified femoral arteries (n=3, approximately 5–8 mm) explanted after limb amputation (approved by IRB as discarded tissue with patient consent), were scanned first using microCT and then placed in 30 mg of nanoparticle suspension and kept on an orbital shaker at ~200 rpm for 72 hours. After 72 hours of incubation, the arteries were scanned with microCT to visualize calcification removal. The arteries were then treated again with fresh nanoparticles and incubated for another 72 hours, after which they were scanned with microCT for calcification removal. The procedures involving human experiments were approved by the institutional review board of Health Sciences South Carolina (HSSC) (approval #Pro00106555), and was conducted in accordance with the Declaration of Helsinki (as revised in 2013). Informed consent has been obtained from the patients.

Statistical analysis

At least six animals were randomly assigned to each treatment group. *Ex vivo* ring culture experiments were repeated twice and assayed at least in triplicates. All numerical data from ring culture and animal studies were evaluated by one-way analysis of variance (ANOVA) to assess statistical differences among groups, followed by Student's *t*-test for pairwise comparisons. Results with P values of ≤0.05 (one-tailed test) were used to identify significant differences between the means of treated and corresponding non-treated or control groups. The mean values from all experiments were calculated from the

averages of at least three independent samples and are presented as mean ± standard deviation (SD) except for mRNA expression which are depicted here as mean ± standard error of mean (SEM) for both *in vivo* and *ex vivo*. The statistical analysis of gene expression data was performed using GraphPad prism 10 (GraphPad Software, LLC, USA) and all other analyses were conducted with Microsoft excel (v16.0) (Microsoft Corporation, USA).

Animals were identified by numbers and blinded to the person doing RT-qPCR and ICP analysis.

Results

Nanoparticle characterization

EDTA-HSA-El-Ab NPs were prepared as described in the methods section (Figure S1). The average yield of conjugated nanoparticles was ~51%, with average particle size and zeta potential of approximately 400 nm, and –24 mV, respectively, as measured with a particle size analyzer (Table S2). The high-performance liquid chromatography showed final EDTA loading of approximately 15% in the conjugated nanoparticles (Table S2). EDTA release from conjugated nanoparticles has been observed over 72 hours (14).

Validation of rat CKD model of severe vascular calcification

The conventional adenine model of renal failure and vascular calcification was modified with VitD3 addition as described in the method section to recapitulate extensive arterial calcification (*Figure 1A*). Histological analysis of harvested kidneys from adenine-fed rats showed severe morphological deformities compared to the standard diet-fed controls (*Figure 1B*). The cortex of damaged kidneys was filled with crystals from adenine metabolites. VitD3 administration following adenine feeding aggravated the injury by enhancing inflammatory cell infiltration, calcium-based mineral deposition, and tissue fibrosis. Further morphological changes were observed with tubular dilation and atrophy, dilations in Bowman's capsule, and hyaline protein casts within damaged tubules. With the intermittent adenine feeding followed by VitD3 injections, we achieved severe calcification throughout the arterial tree (*Figure 1C*), and elevated serum creatinine (1.071±0.457 *vs.* 0.237±0.022), calcium (15.475±1.403 *vs.* 10.600±0.424), and phosphorous levels (10.850±2.366 *vs.* 9.350±0.714) (*Table 1*) implicative of CKD. There was also a significant loss in body weight during adenine diet feeding (*Figure 1D*). The average weight of rats following 21 days of adenine feeding was 311.538±20.474 g compared to the average weights of 393±22.464 g in standard diet fed rats.

Nanoparticles targeting the heavily calcified aorta

For nanoparticle targeting efficacy, 5 days after the last doses of VitD3 injections, two rats were injected intravenously with DiR-HSA-El-Ab NPs. The IVIS imaging coupled with microCT imaging (*Figure 2A*) revealed that the formulated nanoparticles successfully targeted damaged elastin in heavily calcified aortas. We have shown such targeting to elastin in arteries in multiple experiments previously (9,13,14).

Targeted EDTA chelation therapy reversed severe aortic and kidney calcification and osteogenesis

Targeted EDTA therapy was started seven days after the last doses of VitD3 injections when severe arterial calcification was established. The microCT imaging of explanted aortas at the end showed extensive calcification throughout the aortic tissue in the Blank-HSA-El-Ab NPs group (*Figure 2B*). EDTA-HSA-El-Ab NPs removed calcification, particularly from the descending or abdominal aortas, and semi-quantification of images by 3D morphometric analysis represents significantly less total calcium content in full-length aortas (object volume, 129.001±37.785 *vs.* 29.815±24.169 mm^3, P=0.0005) (*Figure 2B*). These results are corroborated by decreased alizarin red stains (% positive stain, 0.766±0.436 *vs.* 0.485±0.208, P=0.05) with comparatively less elastin damage in aortic sections (*Figure 2C,2D*). The ICP-MS quantification for total elemental calcium in portions of aortas from Blank- or EDTA-HSA-El-Ab NPs treated animals showed approximately 20% less calcific burden in EDTA nanoparticles group (124.161±34.410 *vs.* 100.520±19.131 µg Ca per mg of dry aorta, P=0.04) (*Figure 2E*).

Moreover, animals treated with EDTA-HSA-El-Ab nanoparticles showed extended survivability compared to the blank NP-treated animals (*Figure 2F*). We have previously shown that non-targeted EDTA loaded nanoparticles (conjugated with irrelevant IgG antibody) or free EDTA were not effective in reversing calcification as they did not target the aortic elastin (9,14), so we did not use those as control groups in this study. We further eliminated the group of animals receiving no nanoparticles, as during model development, we observed progressive calcification in rats that were on an adenine diet and treated

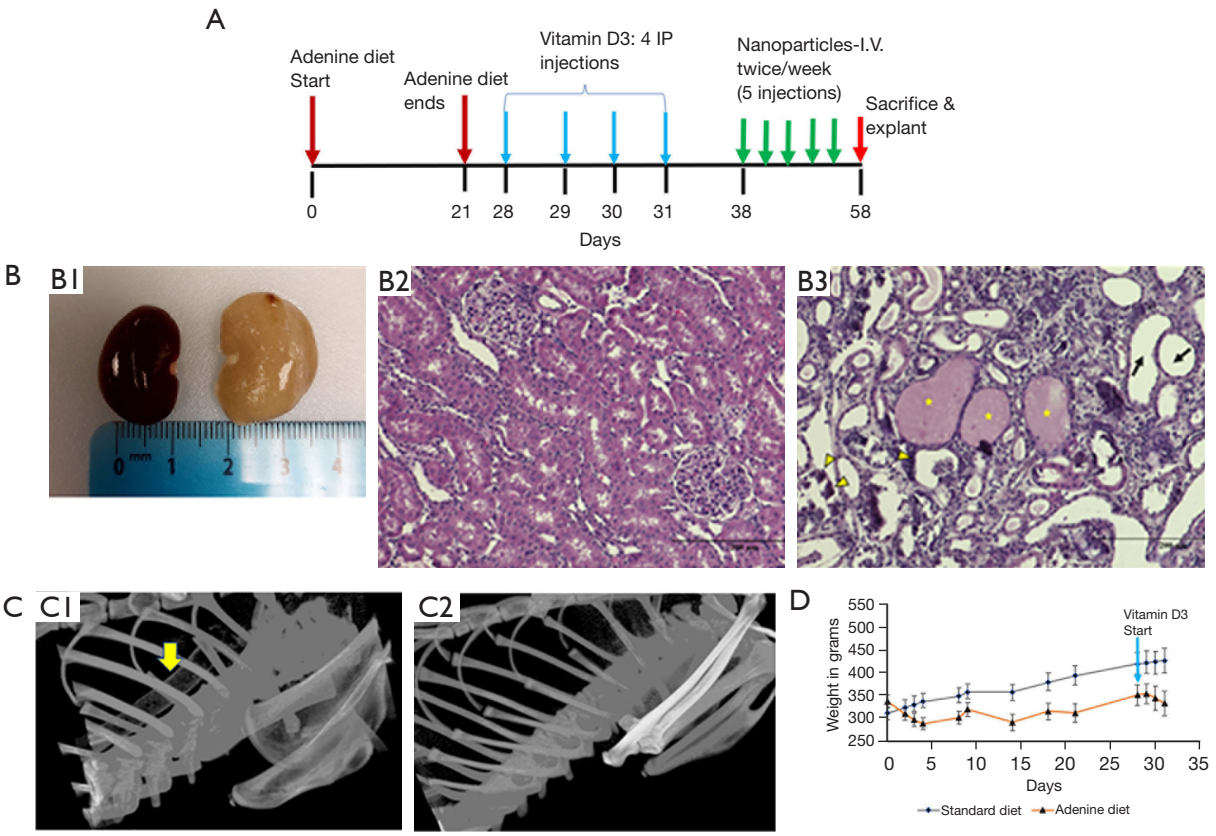

Figure 1 Rat chronic kidney disease model of severe vascular calcification. (A) Schematic diagram of timeline for the calcification reversal study with male Sprague-Dawley rats. (B) Histopathological changes in adenine fed and VitD3 treated kidneys. Representative gross morphology of kidneys from healthy (B1: left) *vs.* adenine and VitD3 treated rats (B1: right). Hematoxylin & eosin staining of corresponding kidney sections (B2,B3). The deposits of adenine metabolite crystals within kidney tubules of combined adenine and VitD3 treated rats are indicated by brown stains; protein casts within necrotic tubular epithelial cells and calcification within damaged tubules are shown with 'star' and 'arrowhead', respectively; tubular dilations are indicated with arrows and inflammatory cells infiltration is notated by dark purple dotted stains. Scale bar: 200 µm. (C) Dual injury with adenine and VitD3 caused severe aortic calcification. Representative microCT images of rats fed adenine diet with subsequent VitD3 treatment (C1) and control fed standard rodent diet (C2). The yellow arrow indicates heavily calcified aorta. Rats were monitored for weight loss during adenine feeding and further during VitD3 injections (D). (N=4 on standard rodent diet, and 26 on adenine diet followed by VitD3). VitD3, vitamin D3; microCT, micro-computed tomography.

Table 1 Serum biomarker analysis

Serum markers	Normal diet (n=4)	Blank-HSA-El-Ab NPs (n=8)	EDTA-HSA-El-Ab NPs (n=9)
Ca (mg/dL)	10.60±0.42	15.47±1.40	16.11±2.29
P (mg/dL)	9.35±0.71	10.85±2.37	11.78±3.95
Creatinine (mg/dL)	0.24±0.02	1.07±0.46	0.80±0.30
ALP (U/L)	25.75±26.47	109.62±43.33	122.22±22.81

Data are presented as mean ± standard deviation. ALP, alkaline phosphatase; EDTA-HSA-El-Ab NPs, anti-elastin antibody conjugated ethylene diamine tetraacetic acid loaded human serum albumin nanoparticles.

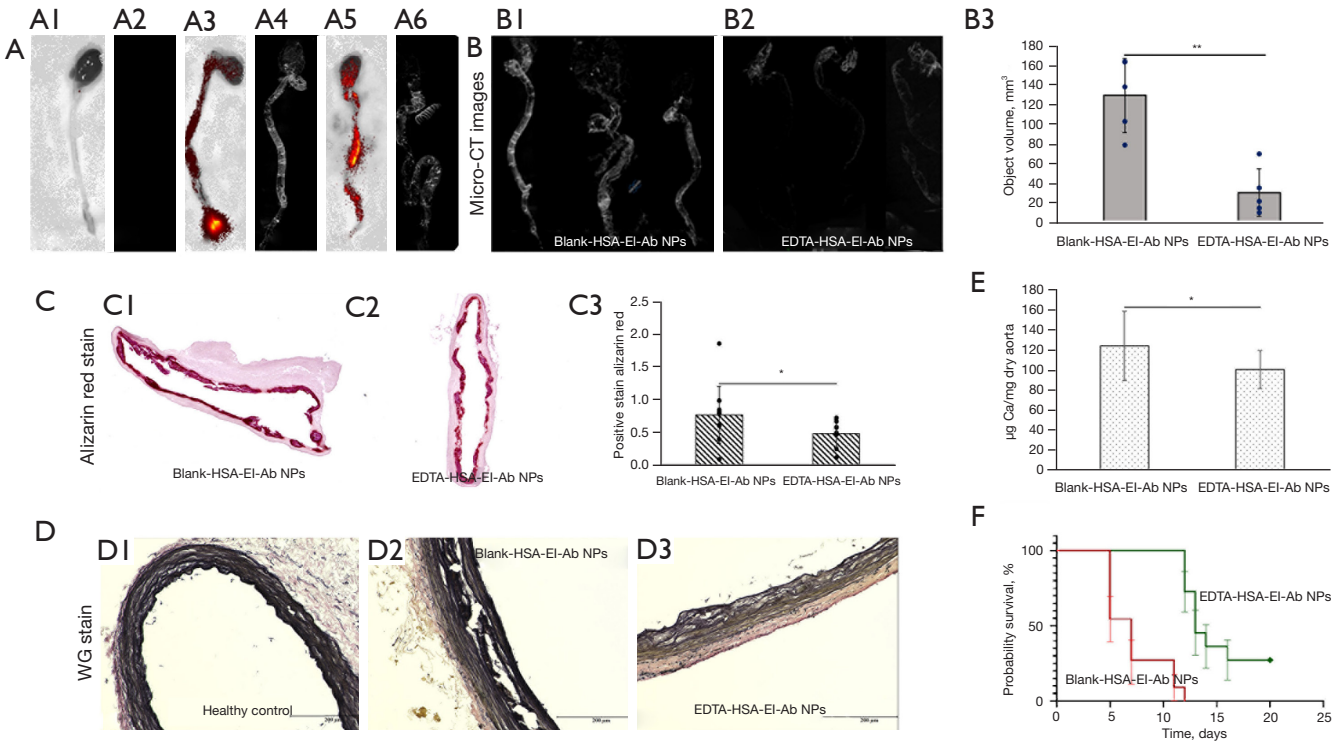

Figure 2 Anti-elastin antibody conjugated EDTA-HSA-El-Ab targeted damaged elastin in the aortas and reversed calcification. (A) Rats intravenously administered with anti-elastin antibody attached DiR-HSA-El-Ab NPs targeted damaged calcified aortic elastin (N=2 per group). Representative IVIS image of adenine fed only aorta (A1); and the aortas from combined adenine and VitD3 treated rats (A3, A5). The adjacent microCT images represent the calcification of respective aortas (A2, A4, A6). (B) Reversal of calcification following targeted nanoparticle therapy. Representative microCT images of harvested aortas from Blank-HSA-El-Ab NPs (B1) *vs.* EDTA-HSA-El-Ab NPs treated group (B2). 3D morphometric analysis was performed on CT scans for semi-quantitative characterization (B3) (N=5 per group). (C) Confirmation of microCT hyperenhancement for calcification on aortic sections. Representative alizarin red staining on aortic sections from Blank-HSA-El-Ab NPs (C1) and EDTA-HSA-El-Ab NPs group (C2). The graph represents the semi-quantification of percentage positive area of stain with alizarin red (C3) (N=8 per group). (D) Aortic elastin damage coexists with calcification. Aortic elastin damages were visualized with VVG staining, Images show elastin architecture in standard chow-fed control (D1) *vs.* Blank- (D2) or EDTA-HSA-El-Ab NPs group (D3). Scale bar: 200 µm. (E) Quantification of total calcium content at termination following targeted therapy. The graph depicts total elemental calcium content following Blank- *vs.* EDTA-HSA-El-Ab NPs therapy (N=4 per group). (F) Survival curve for Blank- *vs.* EDTA-HSA-El-Ab NPs treated animals. Animals that needed to be euthanized for the humane use are included in this curve (N=11 per group). Data represented as mean ± SD. *, P<0.05; **, P=0.0005. EDTA, ethylene diamine tetraacetic acid; microCT, micro-computed tomography; DiR-HSA-El-Ab NPs, DiR-dye loaded human serum albumin nanoparticles; EDTA-HSA-El-Ab NPs, anti-elastin antibody conjugated ethylene diamine tetraacetic acid loaded human serum albumin nanoparticles; HSA, human serum albumin; SD, standard deviation.

with VitD3. We observed severe morbidity and mortality, similar to the group that received blank particles. We believed that blank nanoparticles would be the best control as these particles will target and bind to elastin close to calcification, similar to EDTA-loaded particles, but will not release EDTA. Thus, we can test if EDTA, slowly released from targeted particles, removed calcium.

IHC analysis was performed on the abdominal aortas of each group to assess the expression of genes and proteins—BMP2 and RUNX2—associated with osteogenesis induction. EDTA-HSA-El-Ab NPs significantly suppressed the mRNA expression of both *BMP2* (28.796±15.741 *vs.* 0.318±0.257, P=0.001) and *RUNX2* (4.366±2.959 *vs.* 0.927±0.760, P=0.02) in the abdominal aortas (*Figure 3A,3B*). However, sodium-dependent Pi co-transporter, *PiT-1*, which raises intracellular Pi levels to promote VSMCs calcification,

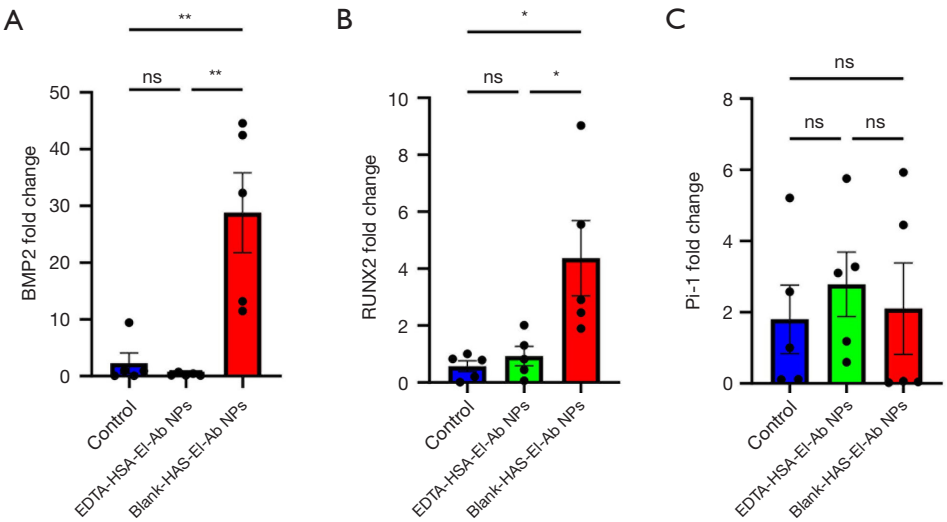

Figure 3 Reversal of aortic osteogenic gene expression following EDTA nanoparticle therapy. Changes in mRNA expression of *BMP2* (A) and *RUNX2* (B) and *PiT-1* (C) in abdominal aortic segments from EDTA-HSA-El-Ab NPs group compared to Blank-HSA-El-Ab NPs or standard chow-fed control. N=5 per group; error bar represents SEM; ns, not significant; *, P<0.05; **, P<0.005. EDTA, ethylene diamine tetraacetic acid; EDTA-HSA-El-Ab NPs, anti-elastin antibody conjugated EDTA-loaded human serum albumin nanoparticles.

showed no differences (2.101±2.867 *vs.* 2.783±2.032, P=0.89) in mRNA expression in EDTA *vs.* blank nanoparticles treated animals (*Figure 3C*).

Proteins expression of BMP2, RUNX2, as well as TNAP, were upregulated in the aortas of animals from Blank-HSA-El-Ab NPs group and brought down significantly (BMP2: 2.935±1.113 *vs.* 1.370±1.338, P=0.01; RUNX2: 1.999±0.937 *vs.* 0.593±0.386, P=0.0005; TNAP: 2.041±0.804 *vs.* 1.195±0.815, P=0.02) by EDTA-HSA-El-Ab NPs (*Figure 4*). Additionally, PiT-1 protein expression was also reduced in EDTA-HSA-El-Ab NPs treated group than the Blank-HSA-El-Ab NPs treated animals (1.109±0.758 *vs.* 0.524±0.734, P=0.08) (*Figure 4*). This clearly suggests that the reversal of calcification is accompanied by suppression of arterial cell osteogenesis.

Further, vitamin D treatment after the adenine diet caused significant calcification in the medullar region of the kidneys (*Figure 5A*). EDTA nanoparticle therapy also cleared kidney calcification, as shown by microCT of whole kidneys (object volume, 24.486±15.062 *vs.* 7.923±11.672 mm^3, P=0.0005) and alizarin red staining for a cross-section (*Figure 5B-5D*). This is expected as a significant portion of nanoparticles also go to the kidneys for clearance. Further, Masson's Trichome staining showed coexistence of mild fibrosis (*Figure 5E*) and supports hyperenhancement from microCT is due to calcification and not fibrosis as the pattern of alizarin red stain closely mimics microCT hyperenhancement.

Finally, cessation of the adenine diet did not cause creatine levels to return to the level observed in control; however, EDTA-HSA-El-Ab NPs slightly reduced the creatinine level than the Blank-HSA-El-Ab NPs -treated animals (shown in Table S1). It is also noticeable that EDTA-HSA-El-Ab NPs did not reduce serum calcium or phosphorous content but increased slightly than the control group, possibly due to their prolonged survival. Furthermore, adenine feeding significantly reduced serum ALP activity in rats compared to standard chow-fed rats or control (147.750±17.153 in adenine fed group *vs.* 252.750±26.474 in control, P=0.0002) (*Table 1*). No differences were noticed in serum ALP activity after EDTA therapy.

To further investigate the efficacy and mechanisms of EDTA chelation for the reversal of severe calcification in the presence of hyperphosphatemia, fresh aortic rings obtained from healthy rats were cultured in high Pi media for ten days to establish heavy mineral deposits in the medial layers, following which aortas were incubated with disodium EDTA while they are still in high Pi medium (*Figure 6A*). The main purpose of the *ex vivo* study was to confirm if EDTA-mediated reversal of calcification follows suppression of osteogenic phenotype as we noticed in our animal study, and to further confirm that it is entirely due to EDTA and not a result of elastin antibody or albumin.

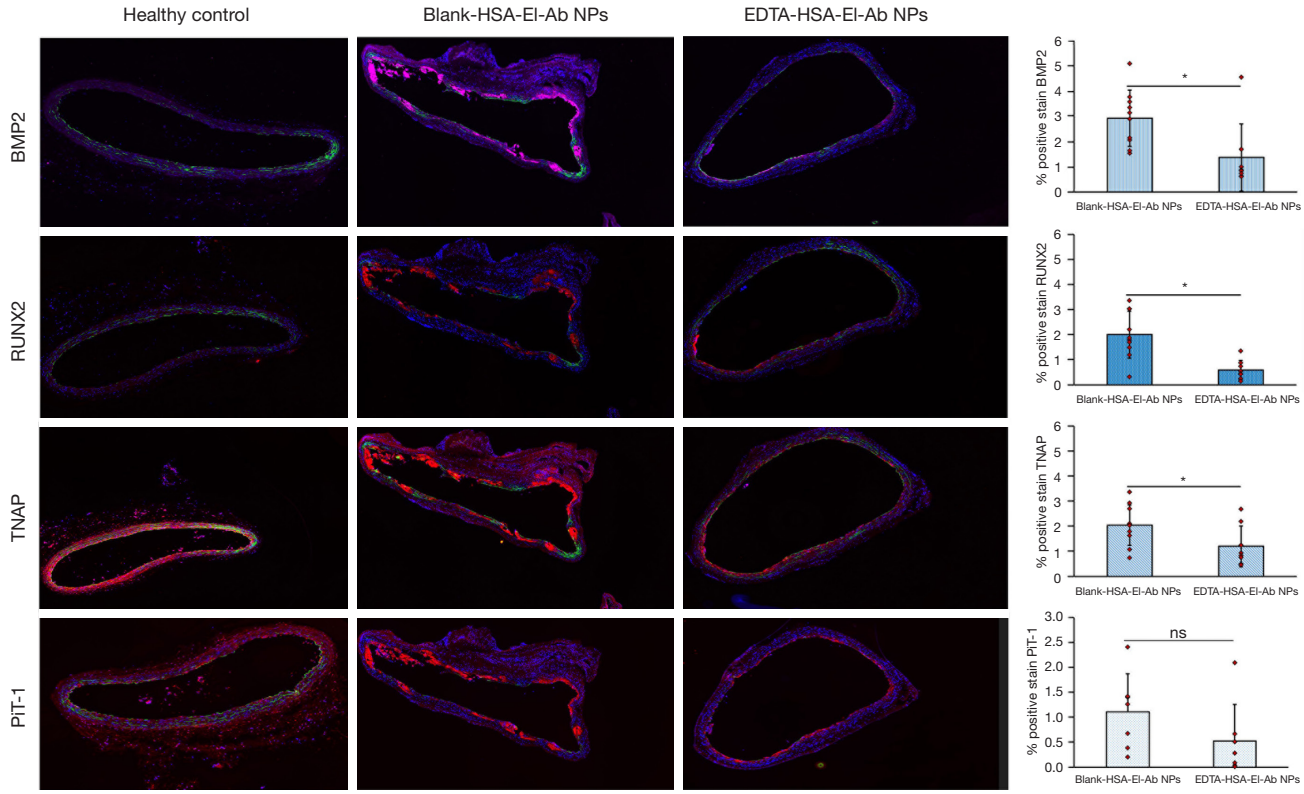

Figure 4 IHC analysis of the aortas for calcification markers. Representative IHC stained images for calcification markers BMP2, RUNX2, TNAP, and PiT-1 following five injections of Blank- or EDTA-HSA-El-Ab NPs; corresponding quantification of percentage positive stain are shown in the adjacent graphs. Red/purple, target proteins; Blue, cell nuclei; Green, elastin autofluorescence. For the semi-quantitative analysis of target proteins, four to six sections of equal spacings were taken from each sample. N=8 per group, error bar represents SD. ns, not significant; *, P<0.05. EDTA-HSA-El-Ab NPs, anti-elastin antibody conjugated ethylene diamine tetraacetic acid loaded human serum albumin nanoparticles; IHC, immunohistochemical; SD, standard deviation.

Thus, we used EDTA alone.

Alizarin red staining showed a significant reduction in calcification in the EDTA-treated group than the non-treated high Pi group (1.654±0.580 *vs.* 0.608±0.250, P=0.02) (*Figure 6B*). Further, the apoptotic marker, caspase-3 expression, was higher in the non-treated high Pi-only group (1.796±1.619 *vs.* 0.350±0.090, P=0.09), indicating enhanced cell apoptosis promoting heavy mineralization (*Figure 6C*).

The osteogenic gene and protein expression in the aortic ring culture study corroborated the findings from the animal study. mRNA levels of *BMP2* (6.697±0.807 *vs.* 1.632±0.368, P=0.004), *RUNX2* (9.716±3.347 *vs.* 3.248±0.364, P=0.03), and *PiT-1* (10.833±2.680 *vs.* 1.360±0.473, P=0.001) are reduced in the EDTA-treated group than in the high Pi-only group (*Figure 7A-7C*). BMP2, RUNX2, and TNAP protein expression decreased after 6 days of incubation with EDTA in high Pi conditions (BMP2: 3.072±1.628 *vs.* 0.624±0.631, P=0.03; RUNX2: 3.626±1.492 *vs.* 1.835±0.932, P=0.07; TNAP: 2.898±0.979 *vs.* 0.657±0.432, P=0.01) (*Figure 8A*, A1-A3). Also, the PiT-1 protein level was reduced after EDTA treatment (0.529±0.880 *vs.* 0.01±0, P=0.18) (*Figure 8A*, A4).

In addition, heavily calcified aortic rings incubated with EDTA for 6 days significantly suppressed the enzymatic activity of TNAP in tissues compared to either high Pi or control group (0.044±0.019 *vs.* 0.006±0.001 ng pNPP per μg tissue protein in Pi *vs.* Pi + EDTA group, P=0.01) (*Figure 8B*). Further, EDTA significantly lowered media TNAP activity following three days of incubation compared to high Pi alone (0.000776±0.000164 *vs.* 0.000356±0.00012, P=0.003) or control groups containing standard Pi (0.000614±0.000168 *vs.* 0.000356±0.00012, P=0.02) (*Figure 8C*). TNAP activity declined further with

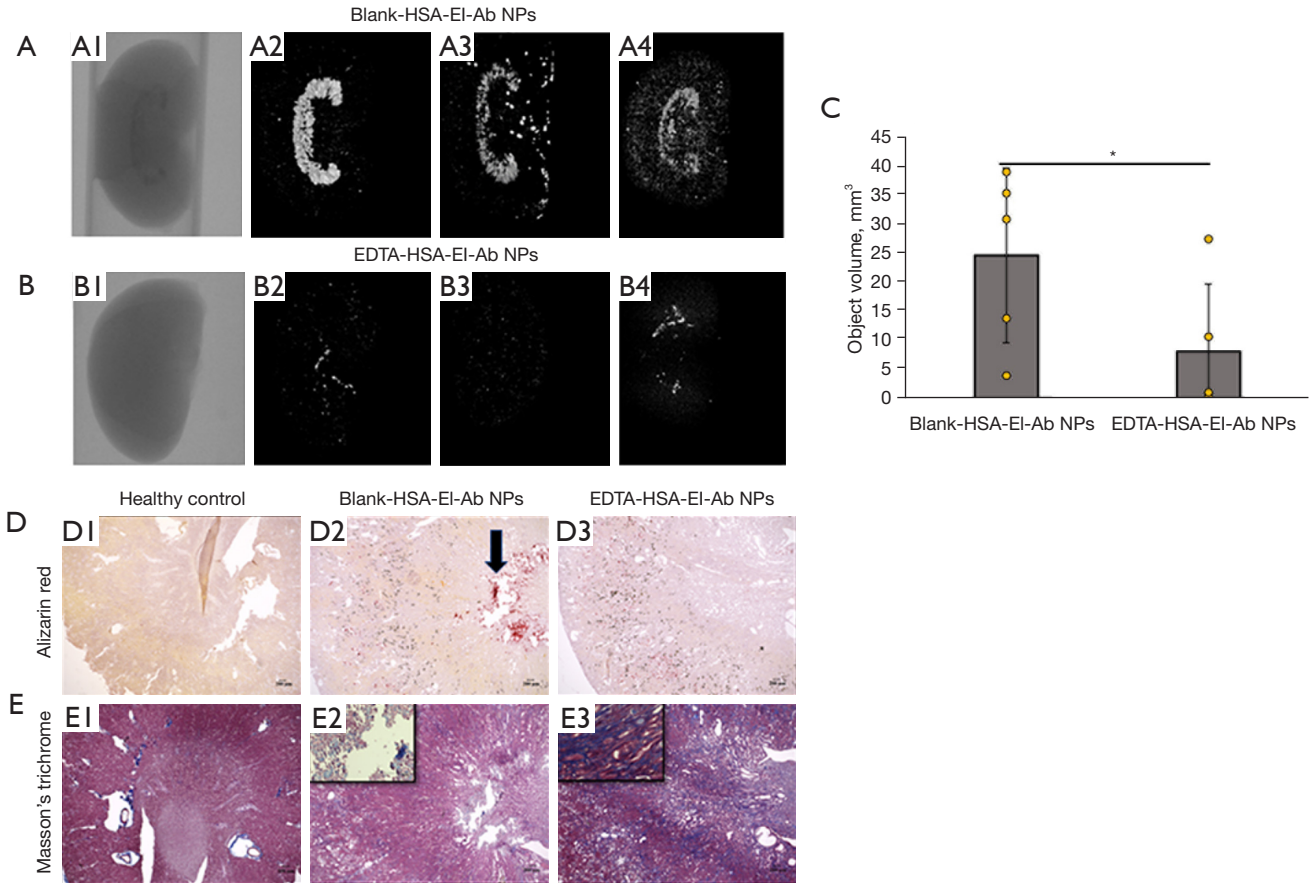

Figure 5 Targeted EDTA therapy reversed kidney calcification. (A,B) EDTA-HSA-El-Ab NPs regressed calcific deposits from kidneys. Representative microCT images of kidneys from animals administered with Blank-HSA-El-Ab NPs (A1-A4) or EDTA-HSA-El-Ab NPs at termination (B1-B4). (C) Quantitative confirmation of CT hyperenhancement. The graph presents 3D morphometric analysis of corresponding microCT scans for semi-quantification of hyperenhancement. N=5 per group; error bar indicates SD; *, P<0.05. (D) Visualization of kidney calcification with alizarin red. Representative alizarin red stains (D1-D3) to confirm calcific deposits in kidneys from control (D1) versus Blank- (D2) or EDTA-HSA-El-Ab NPs treated (D3). The thick black arrow indicates severe calcific deposits in the medulla of Blank group (D2). (E) Coexistance of mild fibrosis with calcific deposits in kidneys. Masson Trichrome stains for collagen deposits in kidney sections from control (E1) and Blank- (E2) or EDTA-HSA-El-Ab NPs treated animals (E3). Scale bar: 200 µm. EDTA-HSA-El-Ab NPs, anti-elastin antibody conjugated ethylene diamine tetraacetic acid loaded human serum albumin nanoparticles; microCT, micro-computed tomography; SD, standard deviation.

6 days of EDTA treatment (Pi: 0.000532±0.000115, Pi + EDTA: 0.000288±0.0000755, P=0.0002). Thus, conforming to animal studies, the aortic ring culture study suggests that EDTA therapy regresses heavy mineral deposits and reverses vascular cell osteogenesis.

Ex vivo decalcification of human arteries with EDTA-HSA-El-Ab

Heavily calcified femoral arteries were collected with consent from patients who went through limb amputation. Arteries incubated with EDTA-HSA-El-Ab NPs for 6 days showed significant reversal of calcification as observed with microCT scanning (untreated: 57.721±28.551 *vs.* day 6 of treatment: 5.441±3.615, P=0.01) (*Figure 9A*) and subsequent alizarin red stains for calcification in arteries (*Figure 9B*).

Discussion

The results from the present study substantiate the hypothesis that EDTA-loaded HSA nanoparticles tagged with elastin antibody that specifically binds to damaged

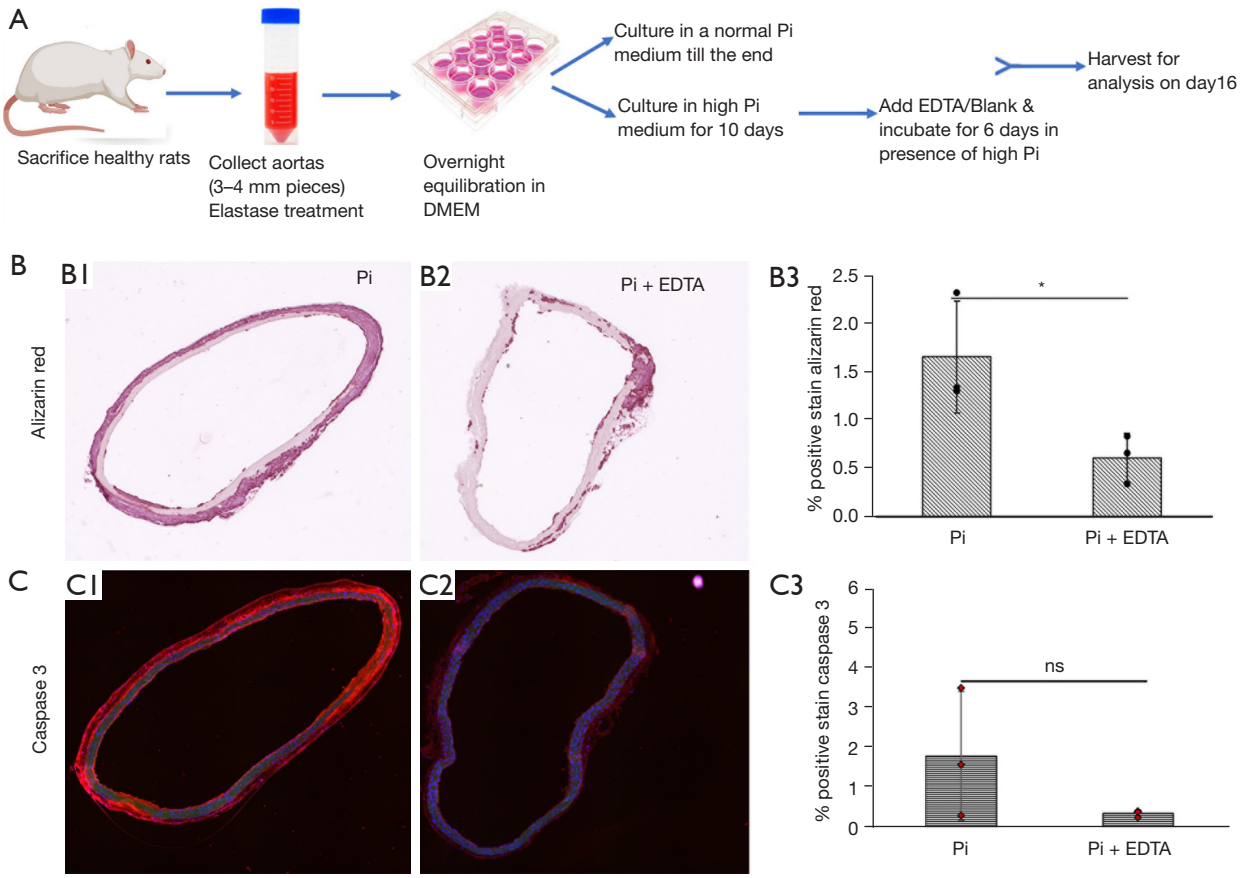

Figure 6 EDTA reversed severe calcification in a ring culture model of rat aortas in presence of hyperphosphatemia. (A) Schematic representation of *ex vivo* aortic ring culture study for the reversal of calcification with EDTA. The image of the sacrifice healthy rat was created with BioRender.com. (B) Histological depiction of calcification removal following EDTA treatment. Representative alizarine red stains on calcified aortic sections after incubation with high Pi alone (B1) or high Pi with EDTA for 6 days (B2). The semi-quantitative data represents percentage positive stain of alizarin red for each group (B3) (N=3 per group). (C) EDTA with selected therapeutic dose and treatment time are non-cytotoxic. Representative immunohistochemical staining for caspase-3 expression for apoptosis in high Pi (C1) compared to combined high Pi and EDTA incubation (C2). The corresponding graph represents semi-quantitative analysis of caspase-3 from stained sections (C3). Red fluorescence indicates caspase-3 expression; blue denotes cell nuclei; and green stain represents elastin autofluorescence. For the semi-quantitative analysis of caspase-3, four to six sections from equal spacings were taken from each sample (N=3 per group). The error bar represents SD. ns, not significant; *, P<0.05. Pi, phosphate; EDTA, ethylene diamine tetraacetic acid, DMEM, Dulbecco's modified eagle medium; SD, standard deviation.

elastin can be targeted to the site of vascular calcification. Further, targeted EDTA therapy substantially reversed heavy arterial and kidney calcification in the modified CKD rodent model and increased animals' survival.

MAC is prevalent in patients with CKD. The clinical parameters associated with MAC in CKD are hyperphosphatemia, secondary hyperparathyroidism (sPTH), and hypercalcemia (6). Hyperphosphatemia and increased calcium-Pi complexes in circulation accelerate MAC (15). The vascular calcification becomes severe as the glomerular filtration rate decreases since the rate of inorganic Pi excretion goes down, which causes serum phosphorous levels to rise. High vitamin D levels further aggravate MAC as it enhances intestinal absorption of phosphorous and calcium, leading to their overload in circulation and bone loss (16). Severe calcification in the medial arterial layer with concurrent bone loss is typical in patients with advanced-stage renal disease (17,18).

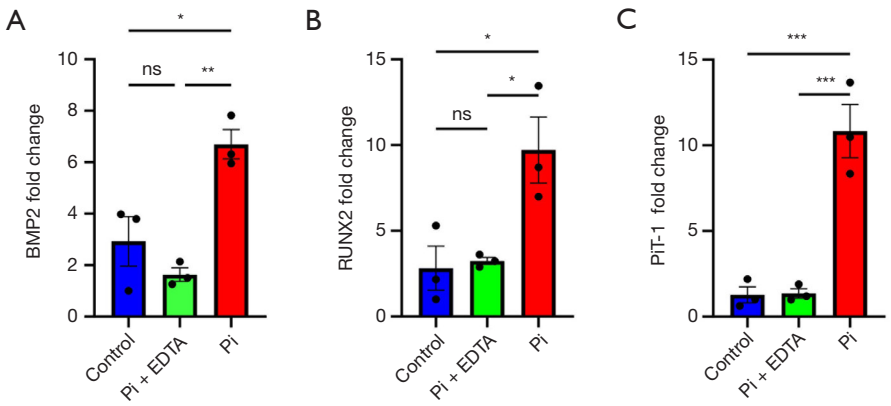

Figure 7 EDTA-mediated reversal of heavy calcification coincided with low expression of calcific genes in aortic rings. mRNA expression of *BMP2* (A), *RUNX2* (B), and *PiT-1* (C) in calcified aortic rings following treatment with high Pi alone or in combination with EDTA for 6 days. N=3 per group; error bar represents SEM. ns, not significant; *, P<0.05; **, P<0.005; ***, P≤0.001. Pi, phosphate; EDTA, ethylene diamine tetraacetic acid; SEM, standard error of the mean.

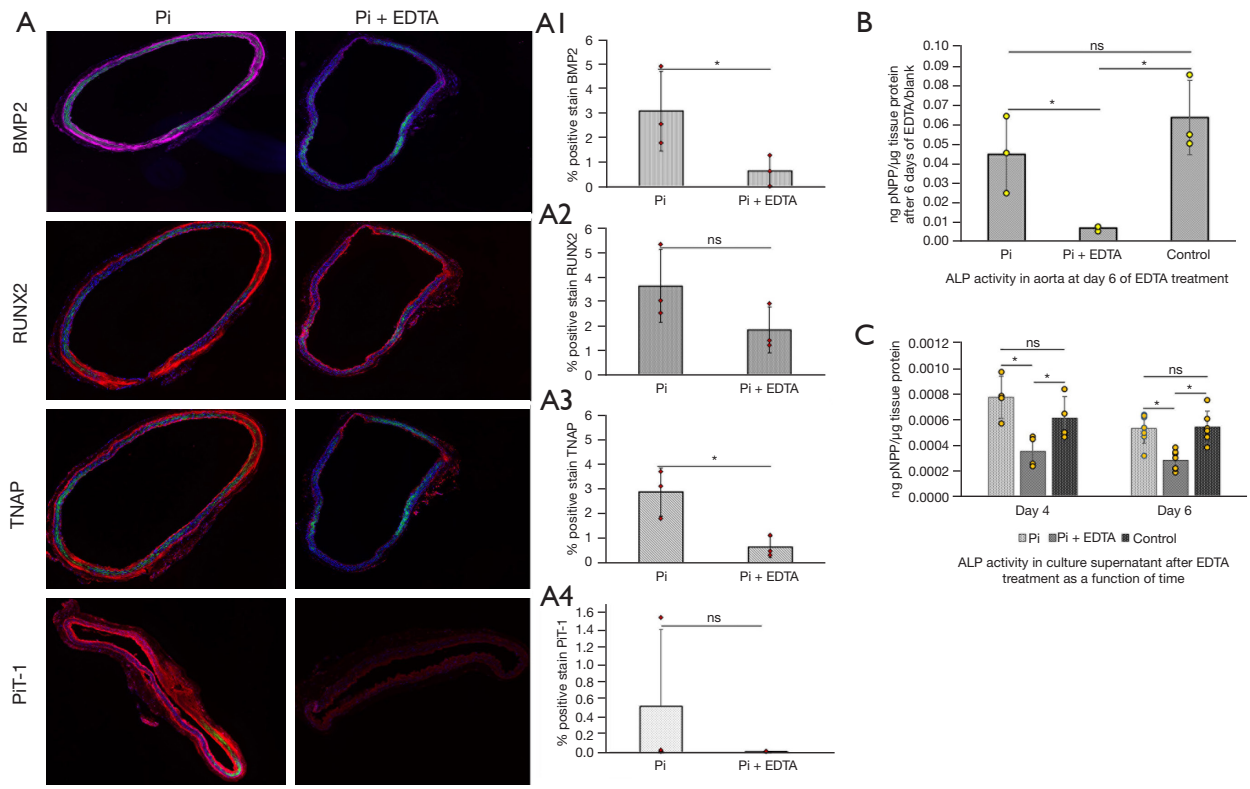

Figure 8 EDTA treatment caused a reversal of osteogenic phenotype. (A) Immunohistochemical analysis of the heavily calcified aortic rings for calcification markers following incubation with EDTA for 6 days. Representative IHC stained images for BMP2, RUNX2, TNAP, and PiT-1 with corresponding semi-quantitative analysis of percentage positive area of stain for each protein (A1-A4) (N=3 per group). Red/purple, target proteins; blue, cell nuclei; green, elastin autofluorescence. For the semi-quantitative analysis of target proteins, four to six sections of equal spacings were taken from each sample. (B,C) Effects of EDTA on ALP enzymatic activity. The graphs represent ALP activity in tissue digests from aortic rings at endpoint (B) as well as culture supernatants from each treatment group as a function of time of EDTA incubation (C). N=3–6 per group. The error bar represents SD. ns, not significant; *, P<0.05. Pi, phosphate; EDTA, ethylene diamine tetraacetic acid; SD, standard deviation; ALP, alkaline phosphatase.

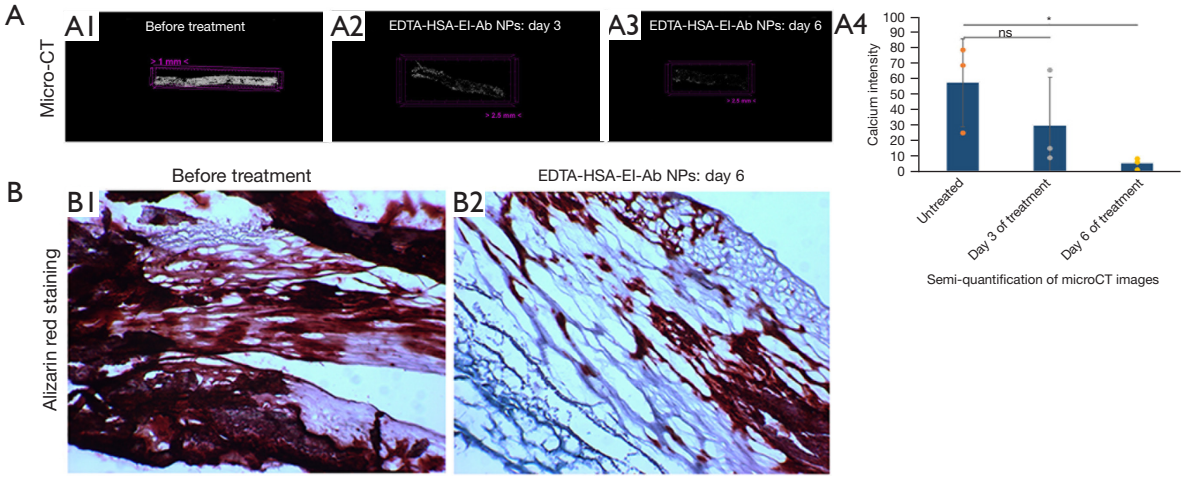

Figure 9 EDTA could reverse extensive human femoral arterial calcification in *ex vivo*. (A) EDTA-HSA-El-Ab NPs reversed severe calcification from human femoral arteries in *ex vivo*. Representative microCT images of arterial segments for CT hyperenhancement following 6 days of incubation with EDTA-HSA-El-Ab NPs (A1-A3). Semi-quantification of microCT images are depicted with bar graph as calcium intensity (A4). (B) Confirmation of CT hyperenhancement for calcification. Representative alizarin red stain to confirm the calcification status from microCT imaging (B1,B2) after EDTA-HSA-El-Ab NPs treatment. N=3 per group; error bar represents SD. ns, not significant; *, P<0.05. EDTA-HSA-El-Ab NPs, anti-elastin antibody conjugated ethylene diamine tetraacetic acid loaded human serum albumin nanoparticles; microCT, micro-computed tomography; SD, standard deviation.

Our previous publication showed that the adenine diet alone caused sporadic focal calcification of the aorta, and nanoparticle therapy reduced it significantly (9). However, the extent of calcification was minimal, and it did not mimic heavy aortic calcification seen in CKD patients. To replicate clinical features of advanced-stage CKD and associated severe arterial calcification, the rats in this study were fed with a 0.75% adenine diet for 21 days, following high doses of VitD3 administration for four consecutive days to stimulate severe calcification in the aorta. In contrast to some other studies (19), where a high dose of adenine feeding (0.75%) caused excessive mortality, our modified CKD rat model with a carefully controlled feeding of 0.75% adenine diet showed no loss of animals during the 21 days of adenine feeding. However, the rats lost significantly more weight than the regular chow-fed cohort, which is usual during adenine feeding and likely due to reduced food intake and renal fluid loss, leading to massive volume depletion and consequent weight loss (20). We performed intermittent adenine feeding (5 days on and 2 days off), which we adopted from our earlier study (9). The adenine and VitD3 dual treatment caused structural damage to the kidneys, elevated serum creatinine, hypercalcemia, and hyperphosphatemia. Moreover, in contrast to the adenine diet only, where serum creatinine, phosphorous, and BUN dropped towards the average level after cessation of 28 days of adenine diet (9), this study with 21-day adenine feeding and subsequent high doses of VitD3 showed constant elevation of serum creatinine, phosphorous, and calcium. Further, the rodent model in this study represents CKD with stages of 2 or 3, based on eGFR values, along with severe calcification in arterial media throughout the aortic tree, thus providing a clinically relevant model for the study of targeted reversal of heavy calcification by EDTA-loaded albumin nanoparticles in CKD milieu.

Albumin nanoparticles conjugated with anti-elastin antibody can recognize damaged elastin in the aortas for targeting. Elastic lamina degradation is a clinical pathology seen in all vascular calcifications. Elastic fiber degradation unveils the amorphous core of elastin and our custom-made antibody that recognizes 20 amino acid sequences in the amorphous elastin (21). We previously confirmed the targeting efficacy of formulated nanoparticles in a local $CaCl_2$ injury model or systemic CKD model (9,14,22,23). Similar elastin degradation was observed in this study, and elastin antibody conjugated nanoparticles targeted the elastin degraded area, which co-existed with calcification as seen by DiR dye-loaded nanoparticles (DiR-HSA-El-Ab NPs). The aortas from 21-day adenine-fed-only rats were negative for DiR signaling, indicating

that non-damaged aortas were spared from nanoparticle targeting. The liver and kidneys also showed high signal intensity in both normal and CKD rats, possibly due to the uptake of nanoparticles by Kupffer cells in the liver and reticuloendothelial clearance in the kidneys. In earlier studies, we observed that nanoparticles entered the medial layer from the adventitial site through the vasa vasorum, which is probably more advantageous than targeting from the luminal site as severe calcification may hinder nanoparticles targeting from the luminal side (12,22).

The dose and frequency of EDTA-HSA-El-Ab NPs were selected based on EDTA loading and release profile. The nanoparticles used for this study had a loading of approximately 15%, and EDTA-HSA-El-Ab NPs released EDTA over 72 hours (14). Additionally, the zeta potential measured using particle size analyzer was roughly –24 mV. Globular albumin is known to have a net negative charge (24). In the last decade with a series of published studies, we showed that nanoparticle formulations (conjugated with DiR-dye) with zeta potential ranging from –20 to –30 mV are able to target damaged elastin and stay to the damaged sites for several weeks (13). Further, in an in-depth study with the same EDTA formulations we used in this study, Lei *et al.* (14) showed particle stability and targeting of damaged elastin.

The decalcification capability of EDTA depends significantly on the type of calcium Pi crystal. The calcium apatite in bone is crystalline hydroxyapatite. However, the rapid onset of calcification in this study, as well as vascular calcification observed in the vast majority of clinical cases, are not bone-like hydroxyapatite as demonstrated in a seminal study by Charles O'Neill and his research group (25). In several studies, we demonstrated that systemic elastin-targeted EDTA-loaded albumin nanoparticles are able to target and reverse calcification locally (9,14,23), and we estimate 10–15% of the intravenous dosage reaches the sites of damaged/calcified elastin. If we deliver 10 mg/kg nanoparticles with 15% EDTA and rat weight is 400 g, then it corresponds to delivering 600 µg of EDTA total dose per animal, and 60–90 µg of that EDTA goes to damaged vasculature, suggests that, more than a single injection is required to remove calcium deposits, and we sought to do multiple injections.

Thus, following 3 weeks of EDTA-HSA-El-Ab NPs treatment (5 injections), we observed a significant reversal of calcification from the aortas as well as from kidneys, which was confirmed with *ex vivo* microCT imaging and alizarin red staining. ICP-MS was also performed to quantify elemental calcium content in aortic segments that showed 20% reduction in calcification by EDTA nanoparticle therapy. The calcium values in this study are six-fold higher than in the previous study by Karamched *et al.* (9) due to the severity of calcification throughout the aorta in this adenine & VitD3 dual insult model.

Despite having higher serum calcium and phosphorous levels than the other groups, the EDTA nanoparticle-treated group showed less calcium content in the aortas and kidneys. With the size of roughly 400 nm, the particles are big enough to pass through the glomerular filtration barrier (GFB), though it is plausible the GFB sieve were disrupted due to adenine crystallization and VitD3 mediated renal toxicity. We do not claim that our particles targeted the kidney calcification; like most nanoparticles, they go to the kidneys for reticuloendothelial clearance. Perhaps the particles are broken down in kidneys as albumin is degradable, and the dissociated EDTA, which has a size range of approx. 2–4 nm are capable of passing through the filtration barrier. We evaluated the kidney function in all groups at the end of the study by assessing blood biochemistry and found reduced creatinine levels in the EDTA-HSA-El-Ab NPs group, possibly due to clearance of kidney calcification and increased blood flow. However, adenine metabolite crystals were still present in the renal cortex.

Serum calcium and phosphorous levels in the EDTA-HSA-El-Ab NPs treated group were not significantly different from the Blank-HSA-El-Ab NPs group, suggesting that EDTA therapy does not cause systemic hypo or hypercalcemia. Moreover, the animals in the EDTA nanoparticles group survived longer than the control group, possibly due to less calcific burden. Although we did not inject EDTA alone in this study, previously, we showed that systemic injections of EDTA alone (3 mg/kg of body weight) were not as effective (9), suggesting higher concentration and frequent doses are necessary to achieve reversal of heavy calcification, which may elicit systemic side effects as previously confirmed by other researchers (26-28). Targeting EDTA to the site of damage is an attractive alternative to harness its therapeutic potential and, at the same time, circumvent the side effects seen during its non-targeted therapeutic use.

Reversal of calcification was also accompanied by reduced expression of osteogenic markers: BMP2 and RUNX2. BMP2 is an essential regulator of bone formation. Accumulated evidence suggests that BMP2 is critical in vascular calcification since pathologic vascular calcification and physiologic bone formation share similar

molecular mechanisms. Overexpression of BMP2 has been observed in calcified human atherosclerotic lesions (29). Li *et al.* (29) showed that, under high-Pi conditions, BMP2 dose-dependently enhanced human smooth muscle cells (hSMCs) calcification via stimulating sodium-dependent Pi transporter protein PiT-1 for increased Pi uptake. The researchers also found that BMP2 triggers RUNX2 expression, a primary transcription factor for osteogenic differentiation, and inhibits SM22 expression for phenotypic switching to osteoblasts in these hSMCs. Previously, we showed a significant reduction in alpha-smooth muscle actin staining in the calcified aorta and its partial restoration after EDTA therapy (9). The current study found a significant reduction of BMP2 and RUNX2 in the aortas of animals treated with EDTA-HSA-El-Ab NPs. These *in vivo* findings were reinforced by aortic ring cultures where EDTA in the presence of high Pi showed regression of aortic calcium content with low expression of BMP2 and RUNX2 than the non-treated high Pi control group. Animals treated with EDTA nanoparticles also expressed less PiT-1 protein than the sham group. In line with this, *ex vivo* EDTA-treated aortas also showed reduced PiT-1 protein and gene expression than the non-treated ones.

Likewise, EDTA therapy suppressed TNAP that belongs to the family of ectonucleotidases and regulates arterial calcification via hydrolyzing pyrophosphate (PPi) into inorganic Pi, thereby disrupting PPi/Pi homeostasis. A high Pi in serum, called hyperphosphatemia, is the 'most potent' inducer of arterial media calcification, whereas PPi inhibits Pi from incorporating into hydroxyapatite crystals to stop crystal growth (30). TNAP is encoded by a gene named ALP. It is one of the critical enzymes for bone mineralization, and data suggest that it is the ability of TNAP to hydrolyze and reduce PPi levels, rather than generating Pi, that promotes hydroxyapatite formation (30). That means tissue PPi levels are primarily determined by TNAP. High TNAP and low plasma PPi levels have been reported in hemodialysis patients (31). Our study found low TNAP protein expression in rats treated with EDTA-HSA-El-Ab NPs in the aortas compared to those treated with Blank-HSA-El-Ab NPs. Similar results were observed in *ex vivo*, where EDTA significantly suppressed TNAP expression compared to the non-EDTA-treated control groups.

Given that TNAP is an ectoenzyme regulated primarily by alternations in protein expression, similar changes in TNAP activity and protein expression are expected (31). Unsurprisingly, TNAP activity in aortic culture media was significantly lowered after 3 days of incubation with EDTA and decreased further after 6 days of EDTA treatment. The metal (Zn, Mg, Ca) containing the catalytic domain of TNAP faces the extracellular space (32); EDTA chelates those metal ions and suppresses its catalytic activity. Likewise, we observed low total serum ALP activity in all groups in our animal study fed adenine diet; lower ALP is indicative of adynamic bone disease or low-turnover bone disease in the CKD milieu (33), and we demonstrated in our previous study that adenine-feeding causes low bone mass (9). Low serum ALP activity has been assessed in patients with fractures, osteoporosis, and metabolic bone diseases like hypophosphatasia (32,34,35).

In addition, EDTA-HSA-El-Ab NP treatment also decreased mortality compared to the Blank-HSA-El-Ab NP-treated animals, as evidenced by the survival curve. However, the survival curve was contracted based on the animals that needed to be sacrificed due to weight loss of over 25% and clinical signs of suffering for humane end point; thus, the survivability is speculative and more research is needed. Although we did not study the systemic side effects of such therapy, targeted EDTA chelation therapy has previously been demonstrated not to cause any undue side effects on bone metabolism and biomechanics (9,14).

A significant limitation of this study is that this model was very aggressive, and we had to terminate animals due to severe morbidity. Thus, we could not complete our intended six therapeutic dosages of EDTA nanoparticles. All animals from the control group and most from the EDTA nanoparticles group needed to sacrifice before the completion of the study due to severe morbidity, which is probably because of VitD3-mediated persistent toxicity, extensive cardiovascular calcification, and excessive weight loss. Moreover, calcification was still prominent in the ascending aorta or aortic arch region, indicating that more dosages are probably necessary for the nearly complete removal of calcification from all regions of the aortas. We isolated RNA and protein from the whole abdominal aorta, so the gene and protein expression are overall levels in the aorta and not for particular cell types. We need to decipher localized gene and protein expression further.

Conclusions

Since pathological vascular calcification resembles physiological bone formation, finding therapies to reverse vascular calcification without affecting bone metabolism is challenging. To the best of our knowledge, we, for the first

time, showed that anti-elastin antibody conjugated EDTA-HSA-El-Ab NPs can successfully reverse extensive mineral deposits from arteries and kidneys in a rodent model of CKD with extended survivability. The aortic elastin damage is also less severe in EDTA-HSA-El-Ab NPs treated animals. The EDTA in the formulations does not have the ability to reverse damaged elastin. We believe EDTA-HSA-El-Ab NPs therapy prevented further elastin damage from adenine & VitD3 insult and subsequent calcification when the animals were on EDTA nanoparticle therapy. However, our nanoparticle formulation also contains an anti-elastin antibody for targeting, and it is beyond our knowledge if the antibody has some capability for elastin protection/regeneration. In addition, the regression of mineral deposits led to the reversal of osteogenic phenotypes in arterial cells, thus offering an immense possibility of targeted EDTA chelation therapy as a clinical option to treat and reverse severe calcification in CKD patients.

Acknowledgments

We greatly acknowledge the support from veterinary staff at Godley Snell Animal Research Facility (GSRC) at Clemson University and SCBioCRAFT Center.
Funding: This work was partially funded by National Institutes of Health grants (to N.V.) (Nos. R01HL145064, and P30GM131959) and Hunter Endowment at Clemson University.

Footnote

Reporting Checklist: The authors have completed the ARRIVE reporting checklist. Available at https://cdt.amegroups.com/article/view/10.21037/cdt-24-17/rc

Data Sharing Statement: Available at https://cdt.amegroups.com/article/view/10.21037/cdt-24-17/dss

Peer Review File: Available at https://cdt.amegroups.com/article/view/10.21037/cdt-24-17/prf

Conflicts of Interest: All authors have completed the ICMJE uniform disclosure form (available at https://cdt.amegroups.com/article/view/10.21037/cdt-24-17/coif). N.V. reports that this work was partially funded by National Institutes of Health grants (Nos. R01HL145064, and P30GM131959) and Hunter Endowment at Clemson University; has some royalties from Clemson University for Nanoparticle therapy licensed to Elastrin Therapeutics; receives consulting fee as a board member of Elastrin Therapeutics Inc.; has a US Patent for nanoparticle therapy which was issued; holds stocks in Elastrin Therapeutics Inc. and ElastinTech Inc.; and has Founders shares in Annoviant Inc. The other authors have no conflicts of interest to declare.

Ethical Statement: The authors are accountable for all aspects of the work and ensure that questions related to the accuracy or integrity of any part of the work are appropriately investigated and resolved. Animal experiments were approved by the Institutional Animal Care and Use Committee (IACUC) at Clemson University (Animal Use Protocol number 2021-006), in compliance with institutional guidelines for the care and use of animals. The procedures involving human experiments were approved by the institutional review board of Health Sciences South Carolina (HSSC) (approval #Pro00106555), and was conducted in accordance with the Declaration of Helsinki (as revised in 2013). Informed consent has been obtained from the patients.

References

1. Demer LL, Tintut Y. Vascular calcification: pathobiology of a multifaceted disease. Circulation 2008;117:2938-48.
2. Hutcheson JD, Aikawa E. The History of Cardiovascular Calcification. In: Aikawa E, Hutcheson JD, editors. Cardiovascular Calcification and Bone Mineralization. Cham: Springer International Publishing; 2020. p. 3-11.
3. London GM. Mechanisms of arterial calcifications and consequences for cardiovascular function. Kidney Int Suppl (2011) 2013;3:442-5.
4. Albright RA, Stabach P, Cao W, et al. ENPP1-Fc prevents mortality and vascular calcifications in rodent model of generalized arterial calcification of infancy. Nat Commun 2015;6:10006.
5. Nitschke Y, Baujat G, Botschen U, et al. Generalized

arterial calcification of infancy and pseudoxanthoma elasticum can be caused by mutations in either ENPP1 or ABCC6. Am J Hum Genet 2012;90:25-39.
6. Laycock J, Furmanik M, Sun M, et al. The role of chronic kidney disease in ectopic calcification. Cardiovascular Calcification and Bone Mineralization: Springer; 2020. p. 137-66.
7. Lin ME, Chen T, Leaf EM, et al. Runx2 Expression in Smooth Muscle Cells Is Required for Arterial Medial Calcification in Mice. Am J Pathol 2015;185:1958-69.
8. Nahar-Gohad P, Gohad N, Tsai CC, et al. Rat aortic smooth muscle cells cultured on hydroxyapatite differentiate into osteoblast-like cells via BMP-2-SMAD-5 pathway. Calcif Tissue Int 2015;96:359-69.
9. Karamched SR, Nosoudi N, Moreland HE, et al. Site-specific chelation therapy with EDTA-loaded albumin nanoparticles reverses arterial calcification in a rat model of chronic kidney disease. Sci Rep 2019;9:2629.
10. Jono S, Nishizawa Y, Shioi A, et al. 1,25-Dihydroxyvitamin D3 increases in vitro vascular calcification by modulating secretion of endogenous parathyroid hormone-related peptide. Circulation 1998;98:1302-6.
11. Bouderlique E, Tang E, Zaworski J, et al. Vitamin D and Calcium Supplementation Accelerate Vascular Calcification in a Model of Pseudoxanthoma Elasticum. Int J Mol Sci 2022;23:2302.
12. Sinha A, Shaporev A, Nosoudi N, et al. Nanoparticle targeting to diseased vasculature for imaging and therapy. Nanomedicine 2014;10:1003-12.
13. Nosoudi N, Chowdhury A, Siclari S, et al. Systemic Delivery of Nanoparticles Loaded with Pentagalloyl Glucose Protects Elastic Lamina and Prevents Abdominal Aortic Aneurysm in Rats. J Cardiovasc Transl Res 2016;9:445-55.
14. Lei Y, Nosoudi N, Vyavahare N. Targeted chelation therapy with EDTA-loaded albumin nanoparticles regresses arterial calcification without causing systemic side effects. J Control Release 2014;196:79-86.
15. Giachelli CM. The emerging role of phosphate in vascular calcification. Kidney Int 2009;75:890-7.
16. Burt LA, Billington EO, Rose MS, et al. Effect of High-Dose Vitamin D Supplementation on Volumetric Bone Density and Bone Strength: A Randomized Clinical Trial. JAMA 2019;322:736-45.
17. Nickolas TL, Stein EM, Dworakowski E, et al. Rapid cortical bone loss in patients with chronic kidney disease. J Bone Miner Res 2013;28:1811-20.
18. Moe SM. Vascular calcification and renal osteodystrophy relationship in chronic kidney disease. Eur J Clin Invest 2006;36 Suppl 2:51-62.
19. Diwan V, Brown L, Gobe GC. Adenine-induced chronic kidney disease in rats. Nephrology 2018;23:5-11.
20. Dos Santos IF, Sheriff S, Amlal S, et al. Adenine acts in the kidney as a signaling factor and causes salt- and water-losing nephropathy: early mechanism of adenine-induced renal injury. Am J Physiol Renal Physiol 2019;316:F743-57.
21. Vyavahare NR, Rice CD, Nosoudi N, et al. Anti-elastin antibodies and methods of use. Google Patents; 2022.
22. Nosoudi N, Nahar-Gohad P, Sinha A, et al. Prevention of abdominal aortic aneurysm progression by targeted inhibition of matrix metalloproteinase activity with batimastat-loaded nanoparticles. Circ Res 2015;117:e80-9.
23. Nosoudi N, Chowdhury A, Siclari S, et al. Reversal of Vascular Calcification and Aneurysms in a Rat Model Using Dual Targeted Therapy with EDTA- and PGG-Loaded Nanoparticles. Theranostics 2016;6:1975-87.
24. Bert J. The interstitium and microvascular exchange. Handbook of Physiology Section 2: The Cardiovascular System, Microcirculation. 1985:521-47.
25. Han KH, Hennigar RA, O'Neill WC. The association of bone and osteoclasts with vascular calcification. Vasc Med 2015;20:527-33.
26. Pasch A, Schaffner T, Huynh-Do U, et al. Sodium thiosulfate prevents vascular calcifications in uremic rats. Kidney Int 2008;74:1444-53.
27. Guldager B, Brixen KT, Jørgensen SJ, et al. Effects of intravenous EDTA treatment on serum parathyroid hormone (1-84) and biochemical markers of bone turnover. Dan Med Bull 1993;40:627-30.
28. HOLLAND JF, DANIELSON E, SAHAGIAN-EDWARDS A. Use of ethylene diamine tetra acetic acid in hypercalcemic patients. Proc Soc Exp Biol Med 1953;84:359-64.
29. Li X, Yang HY, Giachelli CM. BMP-2 promotes phosphate uptake, phenotypic modulation, and calcification of human vascular smooth muscle cells. Atherosclerosis 2008;199:271-7.
30. Opdebeeck B, Neven E, Millán JL, et al. Chronic Kidney Disease-Induced Arterial Media Calcification in Rats Prevented by Tissue Non-Specific Alkaline Phosphatase Substrate Supplementation Rather Than Inhibition of the Enzyme. Pharmaceutics 2021;13:1138.
31. Lomashvili KA, Garg P, Narisawa S, et al. Upregulation of alkaline phosphatase and pyrophosphate hydrolysis: potential mechanism for uremic vascular calcification.

Kidney Int 2008;73:1024-30.
32. Jackson EK, Cheng D, Ritov VB, et al. Alkaline Phosphatase Activity Is a Key Determinant of Vascular Responsiveness to Norepinephrine. Hypertension 2020;76:1308-18.
33. Kovesdy CP, Ureche V, Lu JL, et al. Outcome predictability of serum alkaline phosphatase in men with pre-dialysis CKD. Nephrol Dial Transplant 2010;25:3003-11.
34. Khandwala HM, Mumm S, Whyte MP. Low serum alkaline phosphatase activity and pathologic fracture: case report and brief review of hypophosphatasia diagnosed in adulthood. Endocr Pract 2006;12:676-81.
35. Alonso N, Larraz-Prieto B, Berg K, et al. Loss-of-function mutations in the ALPL gene presenting with adult onset osteoporosis and low serum concentrations of total alkaline phosphatase. J Bone Miner Res 2020;35:657-61.

Cite this article as: Zohora FT, Arora S, Swiss A, Vyavahare N. Reversal of heavy arterial calcification in a rat model of chronic kidney disease using targeted ethylene diamine tetraacetic acid-loaded albumin nanoparticles. Cardiovasc Diagn Ther 2024;14(4):489-508. doi: 10.21037/cdt-24-17